Y. SENOO

Professor,
Research Institute of
Industrial Science,
Kyushu University,
Fukuoka, Japan. Mem. ASME

M. NISHI

Assistant Professor,
Department of Mechanical Engineering,
Kyushu Institute of Technology,
Tobata, Kitakyushu, Japan

Prediction of Flow Separation in a Diffuser by a Boundary Layer Calculation

From a consideration of flow stability, it is shown that the onset of separation in a diffuser depends upon the local blockage factor. Using performance data for two-dimensional diffusers from the literature, the shape factor of the boundary layer at the separation point H_s is related to the blockage factor B_s at that section, and the formula $H_s = 1.8 + 3.75B_s$ is deduced as the separation-limit relation. It is proved that this separation-limit relation is also applicable to conical diffusers. Furthermore, a simple theory is derived to evaluate the time-mean pressure recovery in the separated region. Using this method, it is possible to predict whether a separation occurs in a diffuser and to evaluate the pressure recovery.

Introduction

The performance of various kinds of fluid machinery and apparatus is limited by flow separation in the passages. Therefore, it is a vital problem in fluids engineering to establish a procedure to predict if and where the separation of flow takes place.

Commonly used separation criteria for steady, incompressible and two-dimensional boundary layers are divided into three groups. The first is based on attaining a skin friction coefficient which is zero at the separation point [1].[1] The second group is based mainly on the pressure distribution of the free stream [2, 3], and the last group is based on shape parameters which characterize the velocity profile in the boundary layer. Though there are various methods to define and evaluate shape parameters such as Buri's method [4], Gruschwitz's method [5], Truckenbrodt's method [6], and Ross-Robertson's method [7], the shape factor $H = \delta^*/\theta$ of von Doenhoff-Tetervin's method [8] is simple and the most widely used. Sandborn [9] proposed a separation criterion based on two parameters: the shape factor H, and the pressure gradient parameter $(\theta^2/\nu)(dU/dx)$. Any one of these methods correctly predicts the separation point with almost the same degree of accuracy for external flows [10]. For internal flow, however, it is said that these predictions are not satisfactory [11].

A literature survey [12] on measured boundary layers inside diffusers shows that the time-mean pressure continues to rise along the diffuser wall even after the shape factor exceeds 1.8, which is often considered to be the separation limit of turbulent boundary layers. In some cases, shape factors over 3.0 have been measured in unstalled diffusers of moderate divergence angle.

There are several factors to show the inapplicability of conventional boundary layer concepts to an internal flow with separation. Near the separation point, the pressure gradient normal to the wall is not negligible and the shear stress near the wall is different from that in ordinary turbulent boundary layers. According to the literature [13] the separation of flow is often unsteady and upstream of a fully separated region is a region of intermittent stall, where the flow is three-dimensional.

It is well known that splitter vanes in a wide angle diffuser considerably improve the performance of the diffuser. Since the distribution of the free-stream velocity is little affected by the vanes, the boundary layer should not be changed much by the vanes. Therefore, it is argued that the improvement of performance due to the vanes is not explained by conventional boundary layer theories. This is another proof that boundary layer analysis has not been considered to be useful for the simple estimation of stalled diffuser performance. Thus, diffuser performance is presently estimated primarily by comparison with existing experimental data [14, 15, 16]. A considerable amount of research on stall and separation has been reported in the literature [11, 17]. Unfortunately, most of the work is qualitative and too complicated to apply in order to derive a simple method for predicting the occurrence and behavior of internal separated flow.

In the present investigation, the incipient stall which is observed at $H = 1.8$ is distinguished from the separation where a large region of low-momentum fluid prevents the free stream from being decelerated. Using the data in the literature [14], the shape factor at the separation point is correlated to the blockage factor at that section. With this correlation, it is possible to use

[1]Numbers in brackets designate References at end of paper.

Contributed by the Fluids Engineering Division and presented at the Winter Annual Meeting, New York, N. Y., December 5–10, 1976, of THE AMERICAN SOCIETY OF MECHANICAL ENGINEERS. Manuscript received at ASME Headquarters, August 16, 1976. Paper No. 76-WA/FE-6.

a conventional boundary layer calculation to predict the location of the separation point and the performance of a diffuser. The present method is simple and crude, disregarding many details of the complex stall and separation processes, but the predictions agree well with time-mean experimental data.

Flow Stability and Separation Conditions in a Diffuser

As shown in Fig. 1, the flow inside a two-dimensional diffuser is assumed to consist of a one-dimensional potential core (free stream) and the boundary layers. If the flow rate is specified as Q, the equation of continuity is

$$Q = U(W - 2H\theta) \tag{1}$$

For a steady, incompressible and two-dimensional boundary layer near the separation point, assuming that the wall friction force is negligible, the momentum integral equation is

$$\frac{d\theta}{dx} + (2 + H)\frac{\theta}{U}\frac{dU}{dx} = 0 \tag{2}$$

It is assumed that disturbances in the boundary layer do not influence the flow upstream beyond a distance ξ. The mean velocity-gradient parameter over the distance ξ is

$$\overline{\frac{\theta}{U}\frac{dU}{dx}} = \frac{\bar{\theta}}{\bar{U}}\frac{\dot{U}}{\xi}$$

where $\dot{U}$ is the difference of U over the distance ξ. If the momentum thickness and the shape factor of one of the two boundary layers at a section increase by $\Delta\theta$ and ΔH due to a disturbance, as shown in Fig. 1, the variation of the free-stream velocity ΔU at the section is derived from equation (1) as follows:

$$\frac{\Delta U}{U} = \frac{H\Delta\theta}{W - 2H\theta} + \frac{\theta\Delta H}{W - 2H\theta} \tag{3}$$ [2]

The variation of the mean velocity-gradient parameter due to the disturbance is described as

$$\Delta\left(\overline{\frac{\theta}{U}\frac{dU}{dx}}\right) = \frac{\Delta\theta/2}{\bar{U}}\frac{\dot{U}}{\xi} + \frac{\bar{\theta}}{\bar{U}}\frac{\Delta U}{\xi} \tag{4}$$

Combining equations (3) and (4)

$$\Delta\left(\overline{\frac{\theta}{U}\frac{dU}{dx}}\right) = \frac{\Delta\theta/2}{\bar{U}}\frac{\dot{U}}{\xi} + \frac{\bar{\theta}}{\bar{U}}\frac{U}{\xi}\frac{H\Delta\theta + \theta\Delta H}{W - 2H\theta} \tag{5}$$

By substituting equation (5) into equation (2), the influence of the disturbance on the increment of momentum thickness is determined. That is,

[2] First time readers will suspect that a factor of 2 is missing in equation (3). The reason is that just one boundary layer has changed as shown in Fig. 1.

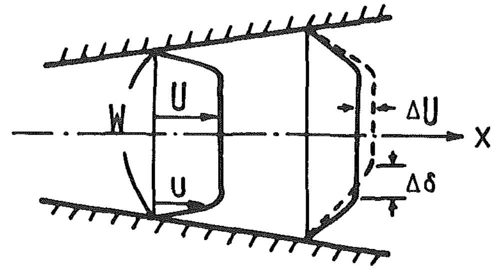

Fig. 1 Flow model of disturbance

$$\Delta\left(\overline{\frac{d\theta}{dx}}\right) = -(2 + \bar{H})\Delta\left(\overline{\frac{\theta}{U}\frac{dU}{dx}}\right) - \Delta\bar{H}\left(\overline{\frac{\theta}{U}\frac{dU}{dx}}\right)$$

$$= \frac{(2 + \bar{H})}{2}\left\{\frac{-\dot{U}}{\bar{U}} - \frac{2H\bar{\theta}/W}{1 - (2H\bar{\theta}/W)}\right\}\frac{\Delta\theta}{\xi}$$

$$+ \frac{\bar{\theta}}{2}\left\{\frac{-\dot{U}}{\bar{U}} - \frac{2(2 + \bar{H})\theta/W}{1 - (2H\theta/W)}\right\}\frac{\Delta H}{\xi} \tag{6}$$

where it is assumed that $\dot{U}/\bar{U}$ is small compared with unity.

If the values in both of the braces of equation (6) are positive, a positive disturbance $\Delta\theta$ or ΔH increases $(\overline{d\theta/dx})$; consequently θ increases further. Therefore a small disturbance grows and the flow may be unstable. If the values are negative, the disturbance decays and the flow is stable to small disturbances. In cases of external flow, the passage width W is infinity and the second terms in each of the braces of equation (6) are zero; consequently, the braces are always positive for decelerating flows and the disturbance grows. In cases of internal flow, the braces may be negative because the second terms in the braces may exceed the first terms.

In a decelerating flow which is about to separate, $(dU/U)/(dx/\theta)$ is of the order of -0.002 [18]. If the distance ξ is of the order of 10θ, then $-\dot{U}/\bar{U}$ is about 0.02, while the second terms in the braces are much larger for most cases of internal flow. Consequently, the disturbance is suppressed. Further, the magnitude of $\Delta(\overline{d\theta/dx})$ from equation (6) is roughly proportional to $H\theta/W$. Thus, this theory shows that the larger $\delta^*/W = H\theta/W$ is, the more stable the flow can be. The free-stream velocity may be decelerated without separation in an internal flow even when the shape factor of the boundary layer exceeds 1.8, providing that δ^*/W is large enough.

In the case of a symmetric two-dimensional diffuser, as shown in Fig. 1, the boundary layers on both diverging walls are identical and $2\delta^*/W$ is the two-dimensional blockage factor at each section of the diffuser. Here, the local two-dimensional blockage factor $B = 2\delta^*/W$ is adopted instead of δ^*/W for the parameter

Nomenclature

- AR = exit/inlet area ratio
- AS = aspect ratio at the inlet section
- B = blockage factor, $= 2\delta^*/W$ for a two-dimensional diffuser, $=2\delta^*/R$ for a conical diffuser
- $C_p(x)$ = local pressure coefficient, $(p - p_i)/(\rho\bar{U}_i^2/2)$
- C_p = pressure-recovery coefficient of a diffuser
- C_p^* = maximum pressure-recovery coefficient for prescribed diffuser length
- H = shape factor, $=\delta^*/\theta$
- N = diffuser length
- p = pressure
- R = radius
- u = velocity in the boundary layer
- U = velocity in the free stream
- $\bar{U}_i$ = mean velocity at the inlet
- W = passage width
- x = distance along the wall
- y = distance from the wall
- δ^* = displacement thickness
- Δ = increment due to disturbance, or increment in the separated layer
- θ = momentum thickness
- ξ = a distance, defined following equation (2)
- 2ϕ = divergence angle of a diffuser

Subscripts

- a = in the separated layer
- i = at the diffuser inlet
- s = at the separation point

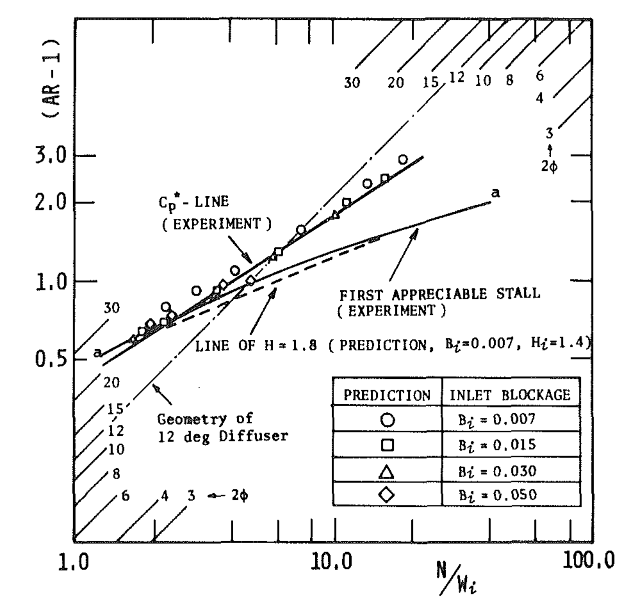

Fig. 2 Comparison of predicted critical geometries for separation (symbols) with the C_p*-line [14] of two-dimensional straight-wall diffusers

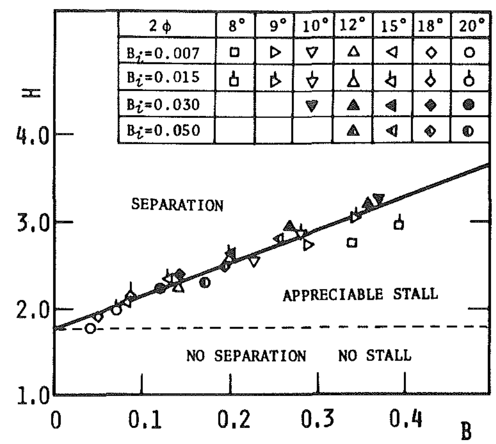

Fig. 3 Calculated relationship between B and H at the exits of two-dimensional diffusers whose geometries satisfy the C_p*-line relation, for the cases of four inlet blockages

used to specify the stability of flow in the diffuser. It is anticipated that, at the separation point, the larger the local blockage factor of a diffuser is, the larger the shape factor at that point will be. In the present study, the correlation between these two parameters will be examined using experimental data.

Separation Limit in a Two-Dimensional Diffuser

Separation-Limit Relation. To study the performance of two-dimensional straight-wall diffusers, Reneau, et al. [14] carried out systematic experiments varying the geometries and the inlet boundary layer thickness and presented a performance chart for each inlet boundary layer thickness. In each of the charts, as shown in Fig. 2, the C_p*-line is drawn to indicate the area ratio where the maximum pressure recovery is obtained for a prescribed diffuser length. It is noted that a single C_p*-line is common to all the charts, i.e., the diffuser geometries indicated by the C_p*-line are the critical geometries regardless of the inlet boundary layer thickness. It is also noted that the C_p*-line is close to the limit of first appreciable stall as defined by line *a-a* of [14].

For a given two-dimensional diffuser geometry and given flow conditions at the diffuser inlet, it is possible to apply a conventional boundary layer calculation iteratively to predict the axial distributions of the free-stream velocity, the boundary layer thickness δ^*, the shape factor H and the blockage B. That is, at first the axial distribution of the free-stream velocity is assumed; then it is adjusted subsequently according to the calculated boundary layer blockage so that the continuity equation (1) is satisfied everywhere. The results may be expected to be valid so long as the boundary layers remain attached.

For a given diffuser length N/W_i, the pressure-recovery coefficient increases as the divergence angle increases unless boundary-layer separation occurs. As C_p* is the maximum pressure-recovery coefficient for a given diffuser length, it is appropriate to assume that the diffuser geometries which achieve C_p* are the critical geometries for separation. That is, the C_p*-line in Fig. 2 indicates the critical geometries for separation, and the line can be used as a reasonable limit of applicability of conventional boundary layer calculation.

For the critical diffuser geometries specified by the C_p*-line, the shape factor H and the blockage B at the exit of the diffusers were calculated using the prediction procedure[3] mentioned above, and it was assumed that these values represented the relationship between H_s and B_s at the separation point. The calculations covered many diffusers with different divergence angles between 8 deg and 20 deg. It was assumed that the shape factor of the inlet boundary layer was 1.4 for all cases, and for each diffuser four alternate inlet boundary-layer thicknesses were treated corresponding to the values reported in [14].

The results are plotted in Fig. 3 with the different marks for the different divergence angles indicated. The calculations are, of necessity, limited to cases where the potential core persists to the diffuser exit. These data are nicely represented by a straight line which intersects $H = 1.8$ at $B = 0$. This line, termed the "separation-limit relation," is expressed as

$$H_s = 1.8 + 3.75B_s \tag{7}$$

In cases of external flows, the blockage factor is zero everywhere, and according to equation (7) H_s is 1.8 which agrees with the value of the conventional criterion for separation. This equation indicates that if the local blockage factor is large in a diffuser, the free stream is decelerated farther downstream without separation even after the shape factor exceeds 1.8.

Flow Which Is Maintained at a Nearly Separating Condition. Using a two-dimensional test section, Spangenberg, et al. [19] adjusted the free-stream velocity so that the boundary layer was almost ready to separate everywhere along the wall, and they measured the velocity profile across the boundary layer at different sections along the test surface. In their experiment, the distribution of the free-stream velocity was controlled by a combination of adjusting the distance of the opposite wall from the flat test surface and by bleeding the fluid through the opposite wall. In this case, the concept of blockage is not applicable for the boundary layer, but an equivalent passage width may be calculated from the distribution of the free-stream velocity, and the blockage factor can be evaluated for the measured boundary-layer thickness.

The measured values H and B at different points along the test surface are plotted in Fig. 4 together with the solid line that represents the separation-limit relation of equation (7). It is seen that all of the measured values of H and B are close to the separation-limit line and none of them are above this line. Thus, this comparison with data further confirms the separation-limit

[3] For the boundary layer calculation a new method [18] was used. For comparison Moses' method was also used and almost identical results were obtained.

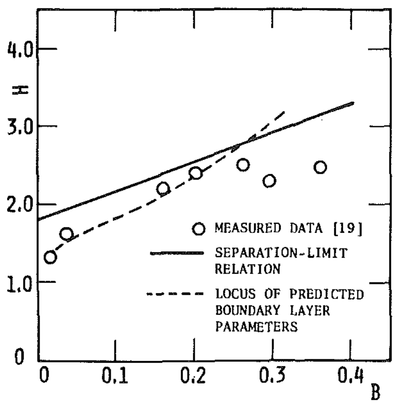

Fig. 4 Relationship between B and H for a flow which is ready to separate everywhere [19]

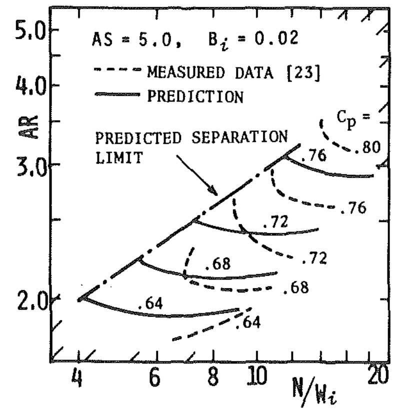

Fig. 5 Predicted and experimental performance chart (constant-C_p lines) of two-dimensional straight-wall diffusers

relation for internal flow. The development of a boundary layer along the test surface was predicted using the boundary-layer calculation procedure and the locus of the calculated boundary-layer parameters is drawn as a dashed line. The line agrees well with the experimental data up to $B = 0.20$. Therefore the boundary-layer calculation procedure is confirmed. It is suspected that at stations farther downstream, the boundary layer fills up the flow passage and the boundary-layer concept based on a potential core is not applicable.

Prediction of Performance of Straight Wall Diffusers. As a check on the method, the boundary-layer calculation procedure was applied to many of the straight-wall diffusers tested in [14] and the critical geometries for separation were calculated using the separation-limit relation of equation (7). The results are plotted in Fig. 2 and lie almost on the C_p*-line as expected regardless of the inlet boundary-layer blockage. The experimental data in reference [14] demonstrate that the C_p*-line in Fig. 2 is universally applicable to two-dimensional straight-wall diffusers with inlet blockage in the range 0.007 to 0.05. Further comparison of the predictions to experimental data with higher inlet blockage was difficult to perform. If B_i is large and 2ϕ is moderate the boundary layer fills up the passage before separation occurs. If 2ϕ is large enough so that the potential core persists at the separation point, the area ratio is small and corresponding experimental data are scarce.

The dashed line in Fig. 2 indicates the diffuser geometry where the calculated[4] shape factor H at the diffuser exit is 1.8 for the initial values of $B_i = 0.007$ and $H_i = 1.4$. The dashed line is very close to line *a-a* which indicates the critical geometries at which first appreciable stall was observed during the flow visualization studies in [22]. From this figure it can be said that the shape factor of 1.8 indicates incipience of stall in internal flows, but the pressure recovery maxima do not occur until H satisfies the separation-limit equation (7).

For a given diffuser, the pressure-recovery coefficient varies depending upon the inlet boundary-layer blockage. In Fig. 5 comparison is made for the cases where the inlet boundary-layer blockage is 0.02. The dashed lines indicate experimentally observed lines of constant pressure-recovery coefficients for various diffusers in reference [23]. The solid lines are the predicted lines of constant pressure-recovery coefficients based on the boundary-layer calculation, and the dash-dot line indicates the separation-limit. The discrepancy of the predicted values of C_p from the experimental values is less than two percent, roughly the data uncertainty, and except for very short diffusers the predicted critical diffuser geometry for separation is very close to the experimentally observed area ratio where C_p is the maximum for a given diffuser length.

Separation Limit in Conical Diffusers

Separation-Limit Relation. An attempt was made to derive a separation-limit relation for conical diffusers similar to equation (7) for two-dimensional diffusers. If a disturbance occurs along one half of the periphery of the axisymmetric diffuser wall, δ^*/R is appropriate as the parameter to specify the stability of diffuser flow. This parameter corresponds to δ^*/W for two-dimensional diffusers. Consequently, it is expected that the separation-limit relation of equation (7) should be applicable to conical diffusers if the conventional definition $B = 2\delta^*/R$ is used.

Flow Conditions in Conical Diffusers. Fraser [24] presented carefully measured data for the turbulent boundary layer developed in a 10 deg conical diffuser and mentioned that the last station No. 10 in Fig. 6(a) was just in the separated region. The measured local pressure coefficients are plotted against the ideal local pressure coefficients of the diffuser in Fig. 6(b). It is noticed that the data points begin to deviate downward at station No. 6 from a straight line corresponding to 0.85 of ideal recovery. It is suspected that a separated layer may cover the last few measuring stations downstream of No. 6. This discrepancy of the location of the separation point from Fraser's explanation may be due to the asymmetric nature of the flow with separation.

The local blockage factor $B = 2\delta^*/R$ and the corresponding local shape factor H were calculated from his measured velocity profile at each of ten stations, and they are plotted in Fig. 6(c). The numbers next to some of these data points indicate the measuring stations in the diffuser as shown in Fig. 6(a). In Fig. 6(c) the measured values of H at the last two stations are just above the separation-limit relation line. Thus, it is demonstrated that the separation-limit relation equation (7) is applicable also to conical diffusers.

The development of B and H along the wall in this 10 deg conical diffuser was predicted using the boundary-layer calculation procedure, and the locus of the results in the B-H plane is shown with a dashed line in Fig. 6(c). The predicted separation condition is taken to be the intersection of the dashed line and the separation-limit line as indicated by S. Concerning the dis-

[4]The new boundary layer calculation method [18] was used for the calculation. Reneau, et al. [20] could not predict line *a-a* for the assumption of H = constant using von Doenhoff-Tetervin's equation. The authors compared the predicted values based on several boundary layer calculation methods for the velocity distributions #3200 and #3800 of reference [21] which were like these of diffusers. Cebeci-Smith's method, Hirst-Reynolds' method, Head's method, Rotta's method, Moses' method, Nash-Hick's method and the present method predicted experimental distribution of boundary layer well, but von Doenhoff-Tetervin's method considerably overestimated the shape factor of boundary layer [21].

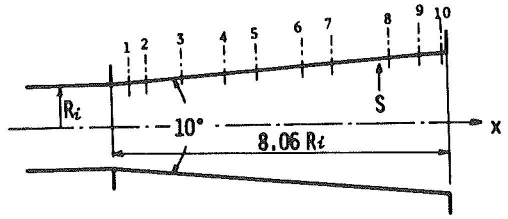

Fig. 6(*a*) Diffuser geometry

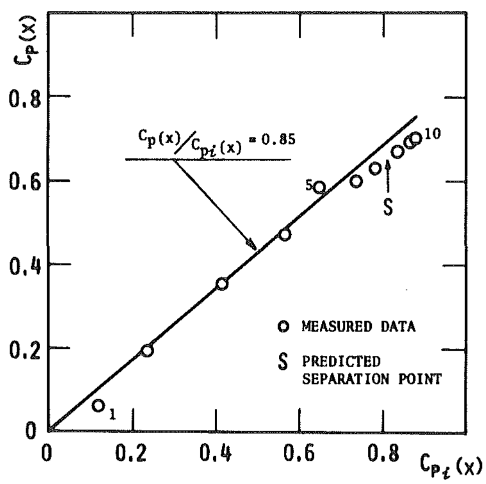

Fig. 6(*b*) Local pressure coefficient

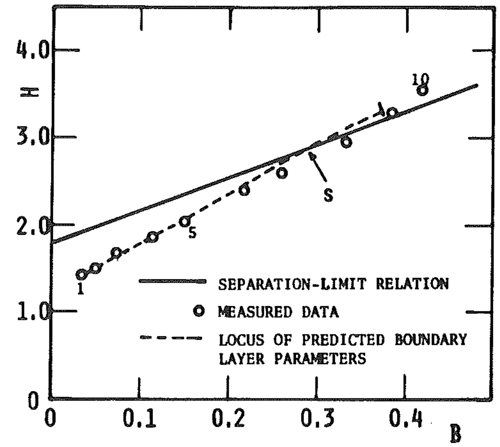

Fig. 6(*c*) Variations of *B* and *H*

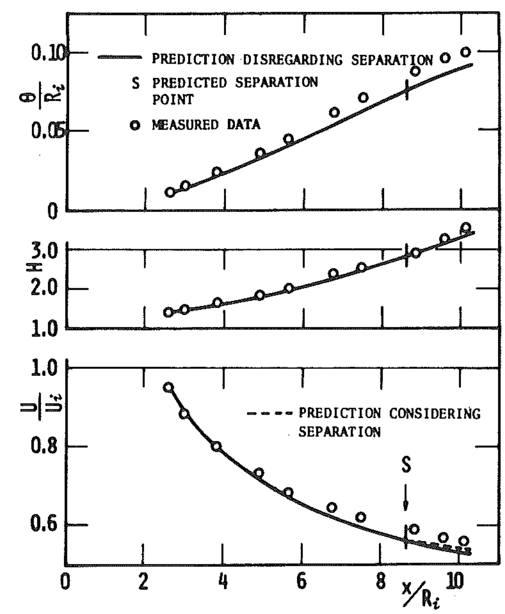

Fig. 6(*d*) Distribution of boundary layer parameters and free-stream velocity

Fig. 6 Comparison of the prediction with experiment on a 10 deg conical diffuser [24]

tributions of core velocity and boundary layer parameters along the wall, the solid lines in Fig. 6(*d*) are the prediction disregarding separation, while the dashed line is the prediction considering a separated layer beginning at *S*. The circles are the experimental data. The prediction method of the core velocity in a diffuser with a separated layer will be mentioned in the next section.

In Fig. 6(*c*) the inclination of the dashed line is not much different from the solid line. Therefore, in the present case a little variation or uncertainty of these two lines causes the location of the predicted separation point to vary considerably. However, as demonstrated in Fig. 6(*d*), the predicted flow conditions are little influenced by small movement of the separation point, because in the case of a small-divergence-angle diffuser the separated layer is thin and considerable pressure rise occurs in the separated region.

A 14 deg conical diffuser with an area ratio of 3.8 was tested by the present authors. In Fig. 7(*a*) the dashed line indicates the predicted locus of the boundary layer parameters *H* and *B* in the diffuser. It is seen that the separation-limit line intersects with the dashed line making a large angle. Therefore, in this case a small uncertainty of the separation-limit line changes the predicted separation point only a little.

In Fig. 7(*b*) the solid line shows the predicted pressure coefficient disregarding separation. The prediction deviates considerably from the experimental values. The dashed line is the prediction assuming that separation occurs at *S*. The agreement with experimental data is much better.

In this case, the prediction overestimates the pressure coefficient slightly near the separation point. One possible reason for the discrepancy is that the separation is three-dimensional and unsteady, and the separation point moves back and forth. Another reason is the imperfection of the prediction method for shape factors that are larger than 2.0, because many prediction methods are derived and adjusted for moderate values of shape factor. Further refinement is needed.

Critical Geometries of Conical Diffusers. With the assumption that the blockage factor at the diffuser inlet was 0.02, boundary-layer calculations were made for five conical diffusers with different divergence angles between 9 and 16 deg. The distributions of *B* and *H* along the wall were calculated for each of these diffusers and the locus of the boundary-layer parameters in the *H-B* plane was drawn. It was assumed that the intersection of this locus and the separation-limit line indicates flow separation, and thus the maximum length without separation for a prescribed divergence-angle diffuser was determined.

The diffuser "critical" geometries determined by this method are plotted with circles in Fig. 8, and the numbers near the circles indicate the corresponding predicted pressure-recovery coefficients. The dashed lines indicate experimentally deduced lines of constant pressure-recovery coefficients [25][5] for many conical diffusers. The agreement with the predicted pressure-recovery coefficients is satisfactory. The solid line is the C_p^*-line that was drawn in reference [16] as the line specifying the optimum area ratio for a prescribed diffuser length. The C_p^*-line does not coincide with the locus of the vertical points of the dashed lines. The discrepancy may be due to the difference of the experimental apparatus and conditions. The circles which indicate the predicted critical area ratio are located near the C_p^*-line and the locus. Therefore, it is concluded that the critical diffuser geometries predicted by the present method are in good agreement with the data.

Pressure Recovery Downstream of Separation Point

It is well known that separation in a diffuser is inherently unsteady and asymmetric and that the influence of separation on the free-stream flow appears even upstream of the separation point. There are many qualitative studies on the nature of stall and separation, but the phenomena are so complicated that detailed quantitative information is scarce [17, 27]. It is commonly assumed that the pressure is constant in a separated region, but according to experiments on diffusers with moderate divergence angles, time-mean pressure sometimes rises downstream of what appears to be the separation point as shown in Fig. 7(*b*).

The geometries of two-dimensional constant-angle diffusers are indicated in Fig. 2 as parallel straight lines with an inclination of 45 deg. For example a dash-dot line indicates the geometry of 12 deg diffuser. The line intersects with the C_p^*-line at $N/W_i = 6$, i.e., separation occurs at $N/W_i = 6$ in the diffuser. Although the pressure-recovery coefficient is not shown in Fig. 2, it is observed in the original drawing [14] that $C_p = 0.7$ at $N/W_i = 6$ and $C_p = 0.74$ at $N/W_i = 14$ for the 12 deg diffuser. That is, there is a pressure rise in the separated region.

In this section, without considering the details of the nature of stall and separation, a steady one-dimensional analysis is applied together with boundary-layer blockage and separation blockage to estimate the free-stream velocity distribution in a diffuser with separation.[6]

Derivation of Prediction Procedure. The momentum integral equation for a boundary layer is applied here to a separated region. Because the wall shear force is negligible in the separated region, the momentum equation is

$$\frac{d(U^2\theta)}{dx} = H\theta \frac{1}{\rho}\frac{dp}{dx} \tag{8}$$

According to this equation, the increment of momentum defect is due to the pressure gradient acting on the boundary-layer displacement thickness. Therefore, the flow field may be simplified by the following model.

The flow consists of a free stream (potential core) and a layer

[5]With regard to experimental data for conical diffusers, reference [15] is better known than reference [25]. One of the authors of the former noted [26] that their pressure-recovery coefficients were lower than many other data. Therefore reference [25] is used here.

[6]In external flows, the free-stream velocity distribution along the wall depends upon the curvature of streamlines. Therefore, the velocity distribution varies considerably due to separation. In the case of diffuser flow, the free-stream velocity distribution along the wall is mainly decided by the effective cross-sectional area of the passage, and the influence of streamline curvature on the velocity distribution is secondary. Furthermore, if the flow separates in a diffuser with a small divergence angle, the curvature of the free stream near the separation point is small. If the divergence angle is large, the curvature is large and the pressure distribution along the wall is locally influenced by the curvature. However, in such cases it is demonstrated in Fig. 7(*a*) that the dashed line intersects with the solid line making a large angle, consequently the location of the separation point does not change much even if the boundary layer develops somewhat differently due to the curvature of the separated streamline. Therefore in the present analysis streamline curvature near the separation point is disregarded.

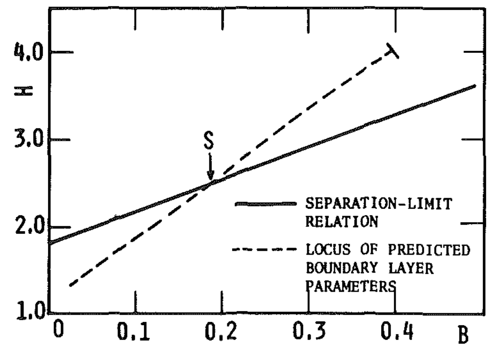

Fig. 7(*a*) Variations of *B* and *H*

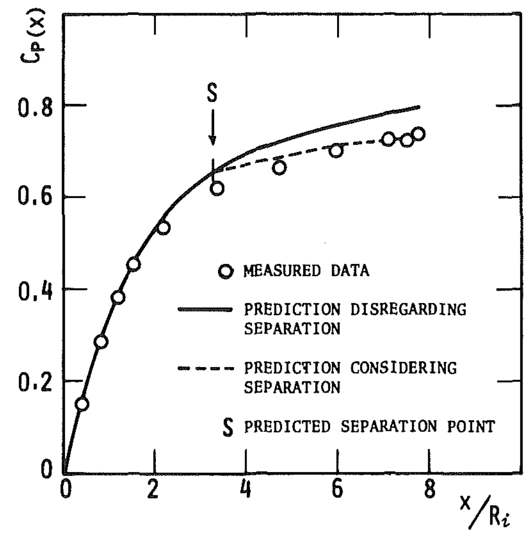

Fig. 7(*b*) Distribution of local pressure coefficient

Fig. 7 Comparison of prediction with experiment on a 14 deg conical diffuser

near the wall where there is no flow (displacement thickness). The pressure force acting on the displacement thickness must be balanced by the shear force acting on the edge of the separated layer, or on the border between the displacement thickness layer and the potential core. The shear force is, in turn, balanced by the increment of the momentum-defect of a part of the core flow, as expressed in equation (8). Therefore, the time-mean pressure rise in the separated region is proportional to the shear force between the separated layer and the potential core.

In the case of a free jet, there is no pressure gradient and the increment of the momentum of the induced flow is balanced by the increment of the momentum-defect of the jet. The amount of momentum exchange depends upon the turbulent shear force acting on the boundary. It may be assumed that the shear stress acting along the edge of the separated layer is almost identical to the shear stress along the boundary of the jet flow and the induced flow. The shear stress is represented by the maximum shear stress in the shear layer, and the magnitude can be estimated from the experimental data on free jets.

A virtual kinematic viscosity ϵ in a free shear flow is given [28] as

$$\epsilon = 0.014b_{0.1}U \tag{9}$$

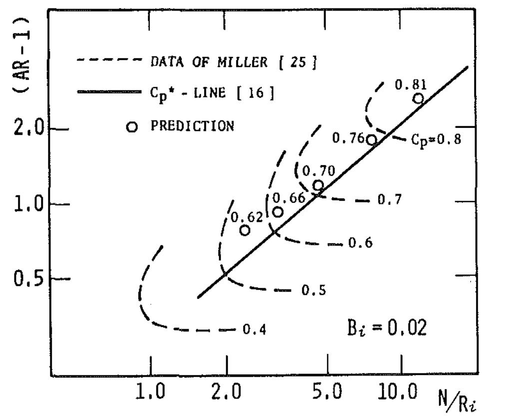

Fig. 8 Comparison of predicted critical diffuser geometries and C_p values with an experimentally determined performance chart [16, 25] of conical diffusers

where $b_{0.1}$ indicates the distance from the position of $(u/U)^2 = 0.1$ to that of $(u/U)^2 = 0.9$. An example of the velocity distribution in the shear layer is presented in Fig. 9 [28]. Since the maximum velocity gradient $|du/dy|_{max}$ is about $0.7U/b_{0.1}$ as indicated in Fig. 9, the maximum shear force τ_m is

$$\tau_m = \rho\epsilon \left|\frac{du}{dy}\right|_{max} = 0.02 \frac{\rho}{2} U^2 \tag{10}$$

With the shear stress along the edge of the separated layer assumed to be identical to the shear stress along the edge of a free jet, the right-hand sides of equations (8) and (10) may be equated. Thus,

$$\delta^* \frac{1}{\rho} \frac{dp}{dx} = 0.02 \frac{1}{2} U^2 \tag{11}$$

It is assumed that separation occurs only on one wall of a two-dimensional diffuser and that it occurs on half of the periphery for a conical diffuser. Hence, the flow in the diffuser is divided into three zones. They are the boundary layer on a wall, the free stream, and the separated layer on the other wall. For the boundary layer on the unseparated wall, an ordinary boundary layer calculation method is applied. For the separated layer, the pressure rise Δp_a from a station 1 to a downstream station 2 is described approximately as

$$\Delta p_a = \frac{\tau_m}{\bar{\delta}_a^*} \Delta x = 0.02 \frac{\rho}{2} U_1^2 \frac{\Delta x}{\bar{\delta}_a^*} \tag{12}$$

where $\bar{\delta}_a^* = (\delta_1^* + \delta_2^*)_a/2$, and δ_a^* indicates the displacement thickness of the separated layer. Bernoulli's equation is applied to the free stream and the following equation is developed:

$$\frac{U_2}{U_1} = \sqrt{1 - \left(\Delta p_a / \frac{\rho}{2} U_1^2\right)} \tag{13}$$

For the case of a conical diffuser, the equation of continuity is

$$U_1R_1(R_1 - 2\delta_1^*) = U_2R_2(R_2 - \delta_2^* - \delta_{2a}^*) \tag{14}$$

For the case of a two-dimensional diffuser with endwalls, it is

$$U_1(W_1 - 2\delta_1^*)(b - 2\delta_{e1}^*) = U_2(W_2 - \delta_2^* - \delta_{2a}^*)(b - 2\delta_{e2}^*) \tag{15}$$

where δ_e^* is the displacement thickness of the boundary layer on the end-walls.

Prediction of the pressure rise from station 1 to 2 follows an iterative procedure:

(1) The velocity ratio U_2/U_1 is assumed.
(2) δ_2^* on the unstalled wall and δ_{e2} on the end-walls are estimated by a boundary-layer calculation method.
(3) δ_{2a}^* is obtained from equation (14) or (15).
(4) Δp_a is calculated from equation (12).
(5) U_2/U_1 is calculated by equation (13).
(6) If the calculated U_2/U_1 does not coincide with the assumed value, the assumed value of U_2/U_1 is corrected and steps (2) through (5) of the calculation are repeated until the difference of U_2/U_1 is less than 0.1 percent.

Comparison With Experiments. The prediction method described above was applied to the 10 deg conical diffuser and to the 14 deg conical diffuser. The results were added in Fig. 6(*d*) and Fig. 7(*b*) as dashed lines. It should be noticed that a considerable pressure rise is achieved in the separated region in the case of the 10 deg diffuser because the displacement thickness of the separated layer is small, but in the case of the 14 deg diffuser the pressure recovery is considerably reduced by the separation, because the displacement thickness of the separated layer increases with the divergence angle.

Comment on Flow Mechanism for a Wide Angle, Two-Dimensional Diffuser With Splitter Vanes

Kline, et al. [29] and Feil [30] have demonstrated that a high pressure-recovery coefficient and stable flow can be achieved with a wide angle two-dimensional diffuser if one or a few short vanes are properly installed at the diffuser inlet. According to conventional boundary-layer theories, the wall boundary layers are little influenced by the vanes as long as the free-stream velocity distribution does not change. Nevertheless, the actual flow behavior is drastically changed by the vanes. Therefore, Kline concluded in reference [13] that conventional boundary-layer theory was not applicable to the prediction of separation in internal flow fields.

Fig. 10(*a*) is a diffuser with a splitter vane. If the flow separates on a wall as shown in Fig. 10(*b*), the flow acquires an incidence angle to the vane and the resulting lift force pushes the flow back to the original condition as shown in Fig. 10(*a*). Owing to this self-controlling effect, the flow along the splitter vane always remains along the extended line of the vane, and in its ability to suppress large transitory stall the vane is equivalent to a virtual wall indicated by the dashed line in Fig. 10(*c*).

If n vanes are installed in a diffuser to divide the inlet portion into $n + 1$ equally spaced portions, the effective diffuser width is about $1/(n + 1)$ times the geometrical width (even downstream of the vanes) and although the wakes of vanes hardly increase the blockage the effective blockage of a wall boundary layer is increased by a factor of $n + 1$. (The stability theory treats the boundary layer on only one wall.) Therefore, the diffuser does not separate even when the shape factor of the bound-

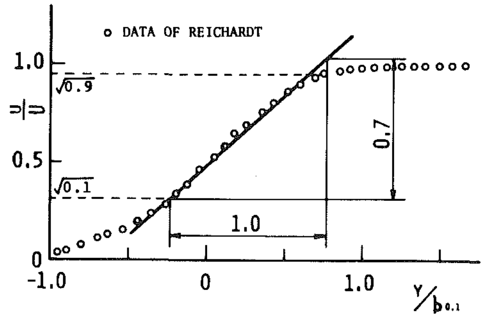

Fig. 9 Velocity distribution in the mixing zone of a two-dimensional jet [28]

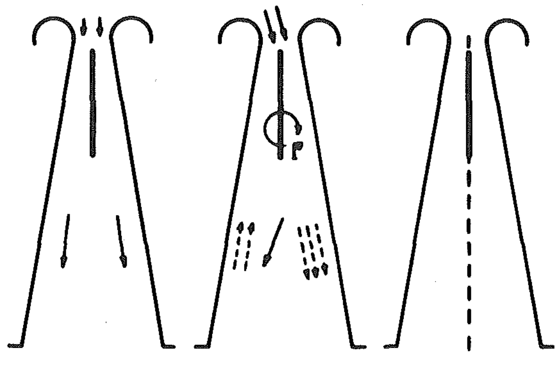

Fig. 10 Effect of a splitter vane on the flow in a wide angle diffuser

ary layer is larger than the value 1.8 required for separation in external flows.

Conclusions

From the present investigation the following conclusions are drawn.

1 The local ratio of the displacement thickness δ^* to the passage width W is the major parameter that controls the stability of flow at that section. The larger the blockage $B = 2\delta^*/W$ is locally, the more stable the flow is, and the less susceptible the boundary layer is to separation.

2 Boundary-layer calculations are applied to two-dimensional straight-wall diffusers that are close to separation at their exits, and the calculated shape factor is related to the calculated blockage factor B_s at the diffuser exit. The separation-limit relation is represented by $H_s = 1.8 + 3.75B_s$.

3 The separation-limit relation is applicable to conical diffusers providing that $2\delta^*/R$ is used as the blockage factor.

4 Using a conventional boundary-layer calculation method and applying the separation-limit relation locally, the separation points in two diffusers were predicted and shown to agree well with experiments.

5 The time-mean pressure rise in a separated region may be evaluated by assuming that a shear stress acts along the edge of the separated layer.

6 Whether diffusers separate or not, it is possible to predict the performance of diffusers by a boundary layer calculation providing that there is a potential core in the diffuser.

7 The agreement of the predicted pressure recovery with the experimental data examined is satisfactory except near the separation point.

8 The influence of splitter vanes installed in a wide angle two-dimensional diffuser is rationally explained by the present theory.

References

1 Cebeci, T., and Smith, A.M.O., *Analysis of Turbulent Boundary Layers*, Academic Press, New York, 1974, pp. 201–202.

2 Stratford, B. S., "The Prediction of Separation of the Turbulent Boundary Layer," *Journal of Fluid Mechanics*, Vol. 5, 1959, pp. 1–16.

3 Goldschmied, F. R., "An Approach to Turbulent Incompressible Separation under Adverse Pressure Gradients," *Journal of Aircraft*, Vol. 2, No. 2, 1965, pp. 108–115.

4 Schlichting, H., *Boundary Layer Theory*, 6 ed., McGraw-Hill, 1968, p. 629.

5 Gruschwitz, E., "Die turbulente Reibungsschicht in ebener Strömung bei Druckabfall und Druckanstieg," *Ingenieur-Archiv*, Vol. 2, 1931, pp. 321-346.

6 Truckenbrodt, E., "Ein Quadraturverfahren zur Berechnung der laminaren und turbulenten Reibungsschicht bei ebener und rotationssymmetrischer Strömung," *Ingenieur-Archiv*, Vol. 20, No. 4, 1952, pp. 211-228.

7 Robertson, J. M., "Prediction of Turbulent Boundary Layer Separation," *Journal of Aeronautical Sciences*, Vol. 24, 1957, pp. 631–632.

8 Von Doenhoff, A. E., and Tetervin, N., "Determination of General Relations for the Behavior of Turbulent Boundary-layer," Report 772, NACA, 1943.

9 Sandborn, V. A., and Kline, S. J., "Flow Models in Boundary-Layer Stall Inception," *Journal of Basic Engineering*, Trans. ASME, Series D, Vol. 83, No. 3, 1961, pp. 317–327.

10 Cebeci, T., Mosinskis, G. J., and Smith, A.M.O., "Calculation of Separation Points in Incompressible Turbulent Flows," *Journal of Aircraft*, Vol. 9, No. 9, 1972, pp. 618–624.

11 Chang, P. K., *Separation of Flow*, Pergamon, 1970.

12 Moses, H. L., and Chappell, J. R., "Turbulent Boundary Layers in Diffusers Exhibiting Partial Stall," *Journal of Basic Engineering*, Trans. ASME, Series D, Vol. 89, 1967, pp. 655–665.

13 Kline, S. J., "On the Nature of Stall," *Journal of Basic Engineering*, Trans. ASME, Series D, Vol. 81, No. 3, 1959, pp. 305–320.

14 Reneau, L. R., Johnston, J. P., and Kline, S. J., "Performance and Design of Straight Two-Dimensional Diffusers," *Journal of Basic Engineering*, Trans. ASME, Series D, Vol. 89, No. 1, 1967, pp. 141–150.

15 Cockrell, D. J., and Markland, E., "A Review of Incompressible Diffuser Flow," *Aircraft Engineering*, Vol. 35, 1963, pp. 286–292.

16 Sovran, G., and Klomp, E. D., "Experimentally Determined Optimum Geometries for Rectilinear Diffusers with Rectangular, Conical or Annular Cross Section," *Fluid Mechanics of Internal Flow*, Elsevier, New York, 1967, pp. 270–319.

17 White, J. W., and Kline, S. J., "A Calculation Method for Incompressible Axisymmetric Flows, Including Unseparated, Fully Separated, and Free Surface Flows," Report MD-35, Stanford Univ., May 1975.

18 Senoo, Y., and Nishi, M., "Deceleration Rate Parameter and Algebraic Prediction of Turbulent Boundary Layer," published in this issue pp. 390–395.

19 Spangenberg, W. G., Rowland, W. R., and Mease, N. E., "Measurements in a Turbulent Boundary Layer Maintained in a Nearly Separating Condition," *Fluid Mechanics of Internal Flow*, Elsevier, New York, 1967, pp. 110–151.

20 Reneau, L. R., and Johnston, J. P., "A Performance Prediction Method of Unstalled, Two-Dimensional Diffusers," *Journal of Basic Engineering*, Trans. ASME, Vol. 89, 1967, pp. 643–654.

21 Kline, S. J., Morkovin, M. V., Sovran, G., and Cockrell, D. J., eds., "Vol. 1, Methods, Predictions, Evaluation, and Flow Structure"; and Coles, D. E., and Hirst, E. A., eds., "Vol. 2, Compiled Data," *Proceedings Computation of Turbulent Boundary Layers-1968 AFOSP-IFP-Stanford Conference*, Stanford Univ., Stanford, Calif., 1968.

22 Fox, R. W., and Kline, S. J., "Flow Regimes in Curved Subsonic Diffusers," *Journal of Basic Engineering*, Trans. ASME, Vol. 84, 1962, pp. 303–316.

23 Runstadler, Jr., P. W., and Dolan, F. X., "Further Data on the Pressure Recovery Performance of Straight-Channel, Plane-Divergence Diffusers at High Subsonic Mach Numbers," *Journal of Fluids Engineering*, Trans. ASME, Series I, Vol. 95, 1973, pp. 373–384.

24 Fraser, H. R., "The Turbulent Boundary Layer in a Conical Diffuser," *Proceedings of ASCE*, Vol. 84, No. HY-3, 1958, pp. 1684/1–17.

25 Miller, D. S., *Internal Flow: A Guide to Losses in Pipe and Duct Systems*, BHRA, 1971.

26 Bradley, C. I., and Cockrell, D. J., "Boundary Layer Methods Applied to Internal Fluid Problems," *Proceedings 1970 Heat Transfer and Fluid Mechanics Institution*, Stanford Univ. Press., 1970, pp. 106–110.

27 Wooley, R. L., and Kline, S. J., "A Method for Calculation of a Fully Stalled Flow," Report MD-33, Stanford Univ., November 1973.

28 Schlichting, H., *Boundary Layer Theory*, 6 ed., McGraw-Hill, 1968, p. 690.

29 Kline, S. J., Moore, C. A., and Cochran, D. J., "Wide-angle Diffusers of High Performance and Diffuser Flow Mechanisms," *Journal of Aeronautical Sciences*, Vol. 24, 1957, pp. 469–470.

30 Feil, O. G., "Vane Systems for Very-Wide-Angle Subsonic Diffusers," *Journal of Basic Engineering*, Trans. ASME, Series D, Vol. 86, No. 4, 1964, pp. 759–764.